

Study of large geomagnetic storms (GMSs) and their association with different solar source activities observed during solar cycle 23

L.K. Borker¹, S.K. Khandayat², and S.C. Dubey³,

¹Department of Physics, Govt. College Umariya (M.P.) - 484661 India.

²Department of Physics, Govt. College Nainpur, Mandla (M.P.)

³Department of Physics, SGS Govt. PG College Sidhi (M.P.)-486661, India

Abstract: Geomagnetic storms (GMSs) are stimulated by higher solar wind flow speed (V_{sw}) and by a southward-directed interplanetary magnetic field (IMF B_z). Two kinds of flows dominate the large scale structure of solar wind: corotating flows and transient disturbances. Corotating flows are associated with spatial variability in coronal expansion and solar rotation, whereas transient disturbances are associated with episodic ejections of material into interplanetary space from coronal regions. The high speed streams originated from coronal interaction regions (CIRs) and transient disturbances are mostly caused by fast coronal mass ejections (CMEs). CMEs are the crucial link between solar activity and transient interplanetary disturbances and are responsible for major GMSs. CMEs eject magnetic flux into interplanetary space that produces abrupt increase in the northward component of Earth's magnetic field. There are two types of geomagnetic field variations termed as long-time variation and storm-time variations. The long-term variations are very useful to solar cyclical study of geomagnetic field variation as well as change in polarity of the Sun, climate change, plants growth rate and geological change of Earth's pole. The storm time variations also known as geomagnetic storm deals the various characteristics of GMSs and their connection with solar source activities and interplanetary magnetic fields. These variations are directly affect us and shows adverse effect in satellites, communication system and power losses. In the present study, we have analysed large geomagnetic storms (GMSs) associated with storm time index (D_{st}) decrease of more than 100 nT observed during solar cycle 23 and found 91 geomagnetic storms falling in our selection criteria. We have analyzed different characteristics of above GMSs and their association with different solar source activities.

Keywords: CMEs, CIRs, D_{st} , IMF, GMSs.

I. Introduction

The geomagnetosphere and upper atmosphere can be greatly perturbed by variations in the solar wind caused by disturbances on the Sun. Changes in the orientation of the interplanetary magnetic field (IMF) and major increases in the velocity and density of solar wind particles striking the magnetosphere result in geomagnetic storms (GMSs). GMSs are seen at the surface of the Earth as perturbations in the components of the geomagnetic field, caused by electric currents flowing in the magnetosphere and upper atmosphere. Major GMSs are the most dramatic manifestation of solar terrestrial coupling. They involve the injection of large amounts of energy from the solar wind into the Earth's magnetosphere, ionosphere and thermosphere. Intense GMSs also have major effects on technical systems in space. An important challenge to solar-terrestrial physicist is to understand which solar and interplanetary process caused the geomagnetic activity. There are many solar source activities which are defined as cause of large geomagnetic disturbances as discussed by many authors. The transfer energy and plasma from Sun to Earth is also interesting. Throughout the heliosphere, the solar wind plasma carries embedded within it solar magnetic field lines. The transfer of energy, momentum and mass from the Sun to Earth for a number of solar perturbations under a variety of interplanetary configurations is also a major scientific objective.

Solar output in term of solar plasma and magnetic field ejected out into interplanetary medium consequently create the perturbation in the geomagnetic field. In recent years, these in situ data have resulted in explosive growth in our knowledge and understanding of solar-interplanetary-terrestrial process. There is a variety of development of GMSs and many authors have suggested several solar and interplanetary causes. The magnetic reconnection provides opportunity to enter solar plasma within geomagnetosphere. Considering various latest theories and mechanism, we have analysed large geomagnetic storms associated with D_{st} decrease of more than 100 nT, observed during solar cycle 23 and its various associations.

II. Selection Criteria And Data Sources

In the present analysis, we have sorted out GMSs associated with D_{st} decrease of more than 100 nT, IMF B ≥ 10 nT with time duration greater than 3 hours, during the period 1996-2007. Different types of solar and geomagnetic indices data are available from different solar and geomagnetic observatories world-wide. The International Service of Geomagnetic Indices (ISGI) and ISGI collaborating institutes have continuously published these indices in the form of data series. Some data is directly available on the internet and some is available on request to principal investigator. During the aforesaid period, we find 91 are large GMSs ($D_{st} \leq -100$ nT). A list of all those selected GMSs and their associative properties are summarized in **Table 1**. In the table, Column (1) and (2) presents serial number and observed date of GMSs. Column (3) presents magnitude of GMSs (D_{st} in net). Column (4) presents the associated solar driver of large GMSs. Peak velocity of CME is noted in column (5). Solar flare class, source region and their co-ordinates are given in column (6-8) respectively.

Table 1: The list of 91 large GMSs and their characteristics, observed during solar cycle 23.

Storm No.	Date of storm	D_{st}	Magnitude (nT)	Solar Driver	CME Velocity Km/sec.	Flare Class	Source Region	Source Coordinate
(1)	(2)	(3)	(4)	(5)	(6)	(7)	(8)	(8)
01	23/10/96	-105	CIR	-	-	-	CH	Unknown
02	21/04/97	-120	CME-S	87	No	Unknown	Unknown	Unknown
03	15/05/97	-115	CME-S	464	C 1.3	AR8038	N21W08	N21W08
04	11/10/97	-130	CME-S	293	No	QS	S27W05	S27W05
05	07/11/97	-110	CME-S	785	X 2.1	AR8100	S14W33	S14W33
06	23/11/97	-108	CME-S	DG	C 1.6	AR8108	N20E05	N20E05
07	18/02/98	-100	CME-S	63	No	Unknown	Unknown	Unknown
08	10/03/98	-116	CIR	-	No	CH	S30	S30
09	04/05/98	-205	CME-M	938	X 1.1	AR8210	S15W15	S15W15
				542	C 5.4	AR8210	S19W09	S19W09
				585	M 1.2	AR8210	S18W04	S18W04
				1374	M 6.8	AR8210	S18E20	S18E20
10	26/06/98	-101	CME-M	289	No	QS	S58W05	S58W05
				192	No	AR8243	N15W30	N15W30
11	06/08/98	-138	CME-M	DG	No	DG	DG	DG
12	07/08/98	-108	CIR	-	No	CH	DG	DG
13	27/08/98	-155	CME-S	-	X 1.0	AR8307	N35E09	N35E09
14	25/09/98	-207	CME-S	-	M 7.1	AR8340	N18E09	N18E09
15	19/10/98	-112	CME-S	362	No	QS	N10E10	N10E10
16	08/11/98	-149	CME-M	523	C 5.2	AR8375	N17E01	N17E01
				1119	M 8.4	AR8375	N22W18	N22W18
17	09/11/98	-142	CME-S	1119	M 8.4	AR8375	N22W18	N22W18
18	13/11/98	-131	CME-S	325	No	QS	N18E00	N18E00
19	13/01/99	-112	CME-S	-	No	DG	DG	DG
20	18/02/99	-123	CME-S	-	M 3.2	AR8458	S23W14	S23W14
21	22/09/99	-173	CME-S	604	C 2.8	QS	S21W05	S21W05
22	22/10/99	-237	CME-S	144	No	QS	S26E08	S26E08
23	13/11/99	-106	CME-M	-	-	DG	DG	DG
24	12/02/2K	-133	CME-S	944	C 7.3	AR8858	N22E03	N22E03
25	07/04/2K	-288	CME-S	1188	C 9.7	AR8933	N16W66	N16W66
26	24/05/2K	-147	CME-M	557	C 7.6	AR8998	S15W08	S15W08
				649	C 6.3	AR9004	N20W22	N20W22
27	16/07/2K	-301	CME-S	1674	X 5.7	AR9077	N22W07	N22W07
28	11/08/2K	-106	CME-S	281	C 1.4	Unknown	Unknown	Unknown
29	12/08/2K	-235	CME-S	702	C 2.3	AR9114	N11W11	N11W11
30	17/09/2K	-201	CME-M	1215	M 5.9	AR9165	N14W07	N14W07
				285	C 7.4	AR9165	N12E04	N12E04
				481	M 2.0	AR9165	N12E07	N12E07
				633	C 9.5	AR9165	N13E08	N13E08

31	05/10/2K	-182	CME-M	173	No	Unknown	Unknown
				586	C 5.0	QS	S27E33
32	14/10/2K	-107	CME-S	798	C 6.7	AR9182	N01W14
33	29/10/2K	-127	CME-S	770	C 4.0	QS	N06W60
34	06/11/2K	-159	CME-S	291	No	Unknown	Unknown
35	29/11/2K	-130	CME-M	675	M 3.5	AR9236	N18W24
				671	X 1.9	AR9236	N20W23
				495	No	QS	S30W40
				980	X 4.0	AR9236	N18W38
36	20/03/01	-149	CME-S	271	No	Unknown	Unknown
37	31/03/01	-387	CME-M	942	X 1.7	AR9393	N20W19
				519	M 4.3	AR9393	N16E03
38	11/04/01	-271	CME-M	2411	X 2.3	AR9415	S23W09
				1192	M 7.9	AR9415	S21W04
39	18/04/01	-114	CME-S	1199	X 14.4	AR9415	S20W85
40	22/04/01	-102	CME-S	-	No	Unknown	Unknown
41	17/08/01	-105	CME-S	618	C 2.3	AR9577	N16W36
42	26/09/01	-102	CME-S	2402	X 2.6	AR9632	S16E23
43	01/10/01	-148	CME-S	846	M 3.3	AR9636	N08E19
44	03/10/01	-166	CME-S	509	M 1.8	AR9636	N13E03
45	21/10/01	-187	CME-S	901	X 1.6	AR9661	N15W29
46	28/10/01	-157	CME-M	1092	X 1.3	AR9672	S18W19
				597	C 2.6	AR9675	S13E27
47	06/11/01	-292	CME-M	1810	X 1.0	AR9684	N06W18
				457	No	DG	DG
48	24/11/01	-221	CME-M	1437	M 9.9	AR9704	S14W36
				1443	M 3.8	AR9698	S25W67
49	24/03/02	-101	CME-M	860	M 1.0	AR9866	S10W58
				603	No	AR9871	S21W15
50	18/04/02	-126	CME-S	720	M 1.2	AR9906	S15W01
51	20/04/02	-151	CME-S	1240	M 2.6	AR9906	S14W34
52	11/05/02	-102	CME-S	614	C 4.2	AR9934	S12W07
53	23/05/02	-108	CME-M	1246	C 9.7	AR9948	S25W64
				1557	C 5.0	QS	S22W53
54	02/08/02	-102	CME-M	562	No	QS	N34W36
				360	No	Unknown	Unknown
55	21/08/02	-106	CME-S	1585	M 5.2	AR0069	S14E20
56	04/09/02	-104	CIR	-	-	CH	S15
57	08/09/02	-170	CME-M	1748	C 5.2	AR0102	N09E28
				-	-	-	-
58	01/10/02	-183	CME-S	178	No	Unknown	Unknown
59	04/10/02	-143	CME-S	258	No	QS	S17W17
60	07/10/02	-107	CIR	-	-	CH	S07
61	14/10/02	-102	CIR	-	-	CH	S26
62	21/11/02	-126	CIR	-	-	CH	S04
63	30/05/03	-131	CME-M	1366	X 3.6	AR0365	S11W12
				964	X 1.3	AR0365	S00W17
				509	M 1.6	AR0365	S07W14
64	18/06/03	-145	CME-M	875	No	QS	N22W15
				2053	X 1.3	AR0386	S07E80
65	12/07/03	-118	CIR	-	-	CH	N04
66	16/07/03	-117	CIR	-	-	CH	N03
67	18/08/03	-168	CME-S	378	No	Unknown	Unknown
68	29/10/03	-363	CME-S	2459	X 17.2	AR0486	S16E08
69	30/10/03	-401	CME-S	2029	X 10.0	AR0486	S15W02
70	20/11/03	-472	CME-S	1660	M 3.9	AR0501	N00E18

71	22/01/04	-149	CME-S	965	C 5.5	AR0540	S13W11
72	11/02/04	-109	CIR	-	-	CH	N02
73	04/04/04	-112	CME-S	-	C 3.4	AR0582	N16W10
74	23/07/04	-101	CME-S	710	M 8.6	AR0652	N10E35
75	25/07/04	-148	CME-S	899	C 5.3	AR0652	N02E08
76	27/07/04	-181	CME-S	1333	M 1.1	AR0652	N04W30
77	30/08/04	-126	CME-S	108	No	Unknown	Unknown
78	08/11/04	-373	CME-M	1055	M 5.4	AR0696	N08E18
				653	C 6.3	AR0696	S09E28
79	10/11/04	-289	CME-M	1759	X 2.0	AR0696	N09W17
				1111	M 9.3	AR0696	N09E05
80	18/01/05	-121	CME-M	2861	X 2.6	AR0720	N16W05
				2049	M 8.6	AR0720	N16E04
81	22/01/05	-105	CME-S	882	X 7.1	AR0720	N12W58
82	08/05/05	-127	CIR	-	-	CH	N10
83	15/05/05	-263	CME-S	1128	M 8.0	AR0759	N12E12
84	20/05/05	-103	CME-S	405	C 1.2	AR0759	N13W29
85	30/05/05	-138	CME-S	586	B 7.5	AR0767	S13E13
86	13/06/05	-106	CME-S	377	C 1.4	AR0767	N07E12
87	24/08/05	-216	CME-M	1194	M 2.6	AR0798	S11W54
				2378	M 5.6	AR0798	S12W60
88	31/08/05	-131	CIR	-	-	CH	S12
89	11/09/05	-147	CME-S	2257	X 6.2	AR0808	S10E58
90	14/04/06	-111	CME-S	-	-	-	-
91	15/12/06	-146	CME-S	-	-	-	-
CME-S ~ Single CME/ICME CME-M ~ Multiple CME/ICME QS ~ Quit Sun region				Class of Solar Flares ~ B, C, X and M respectively CIR ~ Coronal holes/coronal interaction region DG/- ~ Data Gap			

III. Association Of Large GMSs During Different Phases Of Solar Cycle 23

On the basis of comprehensive study of above selected 91 large GMSs observed during solar cycle 23, following conclusions are drawn:

- [1] Out of selected 91 large GMSs events, 57% were sudden commencement type and rest 43% were gradual commencement type.
- [2] The long-term behaviour of occurrence of sudden commencement and gradual commencement GMSs haven't significant correlation between the maximum and minimum phases for solar cycle 23.
- [3] Maximum number of sudden commencement GMSs having their initial phase duration lies between 0-2 hr.
- [4] The main phase duration for maximum number of large GMSs lies between 7-12 hr.
- [5] The best recovery phase duration for maximum number of large GMSs lies between 73-96 hr (3-4) days.
- [6] The main phase duration is always less than the recovery phase duration and the GMSs associated with SSC shows faster recovery in comparison to other GMSs that is not associated with SSC. The study of semi-annual variation of GMSs have important role in space weather prediction.
- [7] The semi-annual variation of large GMSs shows nearly a cyclic variation peaking around April and October months. This result is in good agreement with the findings of Russell-McPherron (1973) and Crooker et al (1992).
- [8] In the first half-annual part (January-June), the maximum number of GMSs occurs during equinoctial April and May. During the next half-annual part (July-December), occurrence rate for large GMSs events is higher during solstitial October and November. This result does not agree with the earlier results obtained by Crooker et al (1992).
- [9] It is also found that the 56% large GMSs occurring during equinoctial and solstitial months.

Association of yearly occurrence of large GMSs with yearly mean sunspot number observed during 1996-2007 is shown in **Figure 1**. **Figure 2** shows the occurrence of large GMSs during different phases of solar cycle 22 and 23. During ascending and maximum phase of solar cycle 22, we observed 20 and 50 GMSs, whereas during its declining phase 29 GMSs were observed. During ascending and maximum phase of solar cycle 23, we have observed 23 and 12 GMSs, whereas during its declining phase 56 GMSs were observed. So, the solar cycle 23 is remarkable for occurrence of large GMSs during its declining phase and shows controversial result measured for past solar cycle 22. From the listed GMSs (Table 1) it is seen that out of 11 severe GMSs ($D_{st} \leq -250$ nT) observed during solar cycle 23, 9 were observed during its declining phase. The largest GMS of solar cycle 23 were also observed on its declining phase. This GMS was observed on 20th November 2003 (20:00 UT) with a D_{st} index of -472 nT, A_p index of 300 and K_p index of 8.7. It was caused by CMEs from active region 0501 had a sky-plane speed of ~ 1660 km s⁻¹, but the associated magnetic cloud (MC) arrived with a speed of only 730 km s⁻¹. The MC at 1 AU had a high magnetic field (~ 56 nT) and high inclination to the ecliptic plane.

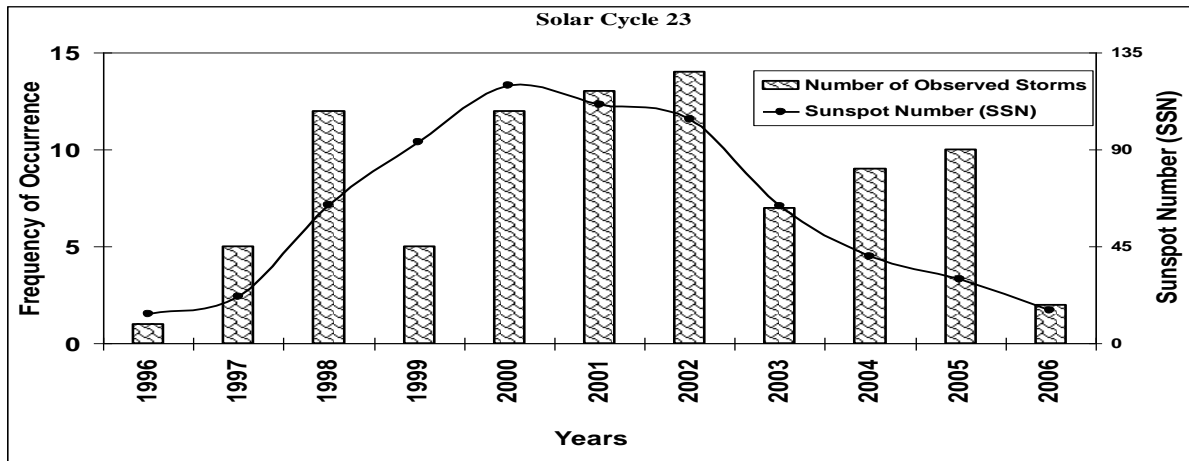


Figure 1: Shows the yearly occurrence of large GMSs and their association With 11-year sunspot cycle, observed during solar cycle 23.

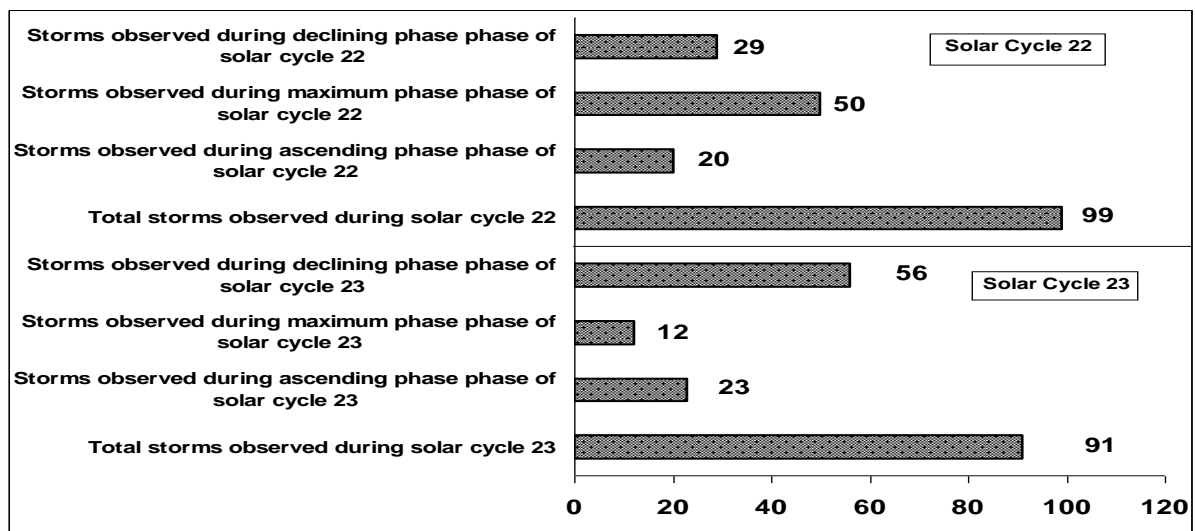


Figure 2: Shows the occurrence of large GMSs during different phases of solar cycle 22 and 23.

IV. Solar Proton Events (SPEs) and Their Impact On HF Communications

Solar Proton Events (SPEs) occurs when high-energy protons are ejected from the Sun's surface during fast solar eruptions and causes geomagnetic and ionospheric disturbances on large scale. These effects are similar to auroral events, the difference being that electrons and not protons are involved. These events typically occur at the north pole, south pole, and South Atlantic magnetic anomaly, where the Earth's magnetic field is lowest. The more severe SPEs events can cause widespread disruption to electrical grids and the propagation of electromagnetic signals. The SPE is the energetic outbursts as a result of acceleration and heating of solar plasma during solar flares and CMEs. The first observation of SPE was recorded by Forbush (1946) in the form of abrupt enhancement in the intensity in ground-level ion chambers during large solar flares that occurred in February and March 1942. The SEPs are classified as the gradual and impulsive. SPEs associated with solar flares are called impulsive where as those associated with CMEs are known as gradual (Cliver, 1983, Cane et al., 1986 and Kahler, 1992).

In the present work, we have studied the general characteristics of SPEs occurred during past solar cycle 23. Occurrence of SPEs are directly associated with fast solar eruptions. Occurrence of fast solar eruptions varies with 11-year sunspot cycle. So, it is important to investigate the association of SPEs with sunspot cycle on long-term basis. In this communication, we have find an association of occurrence of SPEs (energy ≥ 10 MeV) and its two kinds (Impulsive and Gradual) with 11-year sunspot cycle, during solar cycle 23, is plotted in **Figure 3**. These associations haven't shows very significant correlation between the yearly occurrences of SPEs and its two kinds with 11-year sunspot cycle.

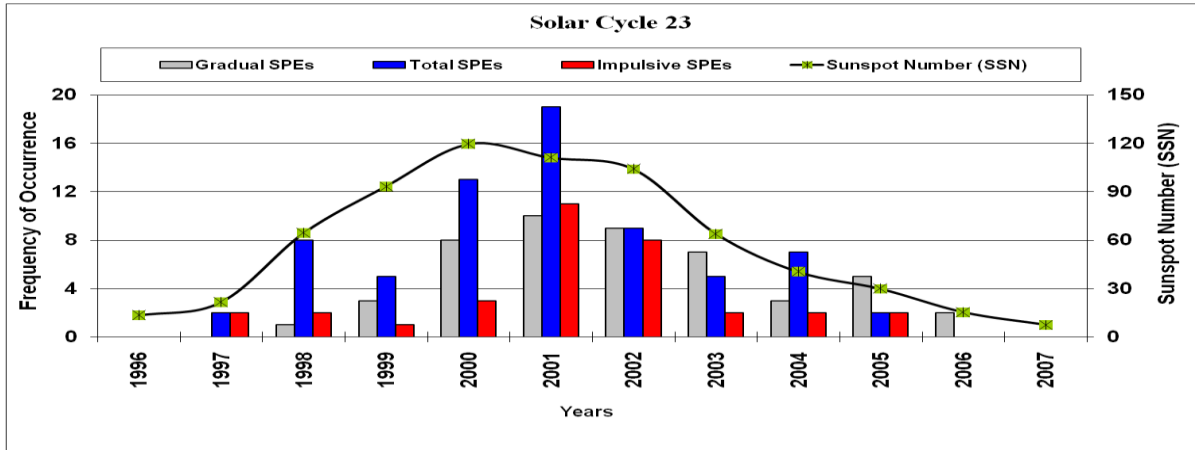


Figure 3: Shows the association of yearly occurrence of solar proton events (SPEs) and their two kinds (Impulsive and Gradual) with 11-year sunspot cycle, observed during the period 1996-2007.

SPEs (energy ≥ 10 MeV) produced by processes at the Sun and interplanetary space arrive at Earth and enter the atmosphere over the polar regions, much enhanced ionization is produced at altitudes below 100 km. Ionization at these low altitudes is particularly effective in absorbing HF radio signals and can render HF communications impossible throughout the polar regions. Space Weather Prediction Center (SWPC) monitors the energetic proton detectors on NOAA’s GOES satellites to determine when an SPE is in progress. The GOES satellite instrument can determine the presence and temporal profile of an SPE, those observations provide no information about the extent of the area over which those protons enter the atmosphere in the polar region or about which radio propagation paths are affected by the increased ionization. NOAA’s Polar Orbiting Environmental Satellites (POES) carry proton detectors similar to GOES. However, each POES satellite transits a polar region twice each orbit and can provide a direct measure of the boundaries and extent of the solar proton fluxes entering the atmosphere during an SPE.

V. Association Of Large GMEs With Halo CMEs And CIRs

In the present section, we have shown the association of selected 91 large GMSs with single front-side halo CME (S-type), multiple front-side halo CMEs (M-type) and corotating interaction region (CIR) (C-type). These associations are shown in **Figure 4**. It is found that 62% GMSs were caused by single front-side halo CME (S-type), whereas 25% GMSs were caused by multiple front-side halo CMEs (M-type). Rest 13% GMSs were caused by corotating interaction region (CIR). We find that there is an east-west asymmetry and north-south asymmetry as well. We have also shown the association of selected 91 large GMSs with three types of surface source region: active region, quiet region and coronal holes, are shown in **Figure 5**. We find that 62% GMSs were caused by active region whereas 10% GMSs were caused by quiet region. 13% GMSs were caused by coronal holes and 15% GMSs are uncertain due to data gap.

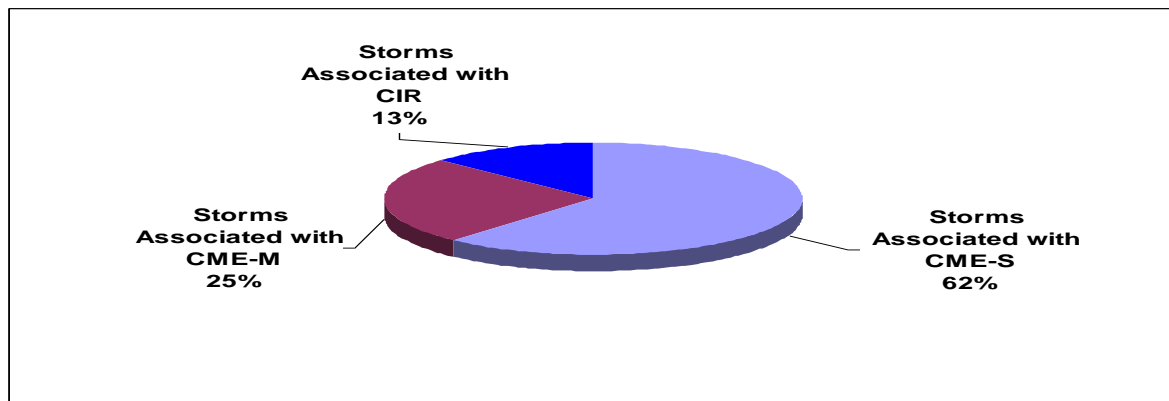


Figure 4: Shows the association of 91 large geomagnetic storms (GMSs) with single front-side halo CME (S-type); multiple front-side halo CMEs (M-type) and corotating interaction region (CIR) (C-type), observed during solar cycle 23.

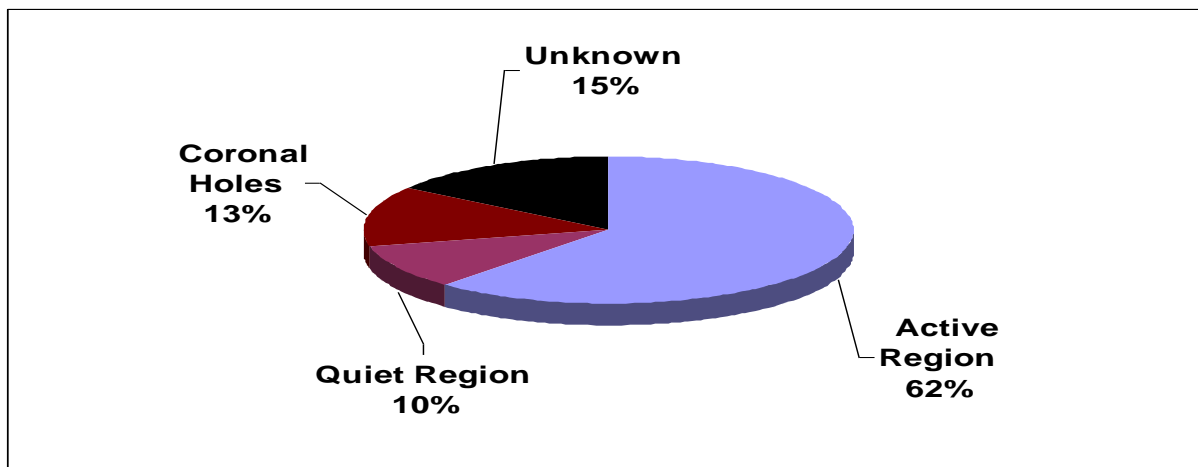


Figure 5: Shows the association of large geomagnetic storms (GMSs) with three types of surface source region: active region, quiet region and coronal holes, observed during solar cycle 23.

VI. Study Of Halo CMEs And Their Geoeffectiveness

CMEs that appear to surround the occulting disk of the observing coronagraphs in sky-plane projection are known as halo CMEs (Howard et al., 1982). Halo CMEs are fast and wide on the average and are associated with flares of greater X-ray importance because only energetic CMEs expand rapidly to appear above the occulting disk early in the event (Gopalswamy et al., 2007). Extensive observations from LASCO/SOHO have shown that full halos constitute ~ 3.6% of all CMEs, while CMEs with width $\geq 120^\circ$ account for ~ 11% (Gopalswamy, 2004). Full halos have an apparent width (W) of 360° , while partial halos have $120^\circ \leq W < 360^\circ$. Halo CMEs are said to be front-sided if the site of eruption can be identified on the visible disk usually identified as the location of H-alpha flares or filament eruptions. Details on how to identify the solar sources are discussed by Gopalswamy et al (2007). Halos with their sources within $\pm 45^\circ$ of the central meridian are known as disk halos, while those with a central meridian distance (CMD) beyond $\pm 45^\circ$ but not beyond $\pm 90^\circ$ are known as limb halos. Disk halos are likely to arrive at Earth and cause GMSs, while limb halos only impact Earth with their flanks and hence are less geoeffective (Gopalswamy et al., 2007).

In the present investigation, we have analyzed in detail all halo CMEs occurred during solar cycle 23. We have considered here two types of halo CMEs. First, the classical full halo CMEs that appears to surround the entire occulting disk very late, often in the field of view of the LASCO/C₃. Sometimes limb events appear as halo due to deflections of pre-existing coronal structures by the fast CME. Therefore, after very careful examination one can distinguish a real halo CME out of limb fast events deflecting coronal material. We have examined the 354 halo CMEs. Here, all CMEs with angular width only 360° have been considered as halo CME. In present section, we have analyzed solar cyclic variation of halo CMEs and its different characteristics.

Out of selected 91 large GMSs occurred during solar cycle 23, 56 were associated with halo CMEs. The largest GMS were observed on 20th November 2003. This event can be put in the category of super GMSs. The D_{st} magnitude during this event is observed to be -472 nt. This event is associated with halo CME from solar active region. Speed of CME is found to be about 1660 km s^{-1} . The histograms of annual distribution of the frequency of halo CME, and their association with annual mean sunspot number is shown in **Figure 6**. We have found that the occurrence frequency of halo CME generally follows the different phases of solar cycle. During the solar maximum the maximum number of halo CMEs have been occurred.

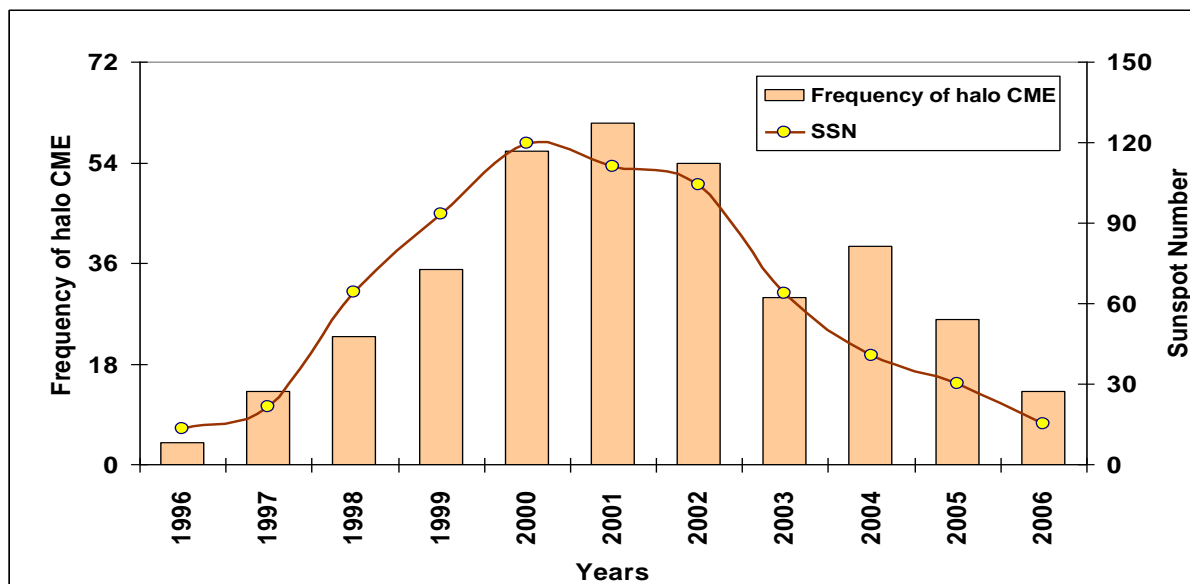


Figure 6: Shows the association of annual frequency of halo CME, and their association with annual mean sunspot number, observed during solar cycle 23.

References

- [1]. Crooker N U, Cliver E W & Tsurutani B T, *J Geophysics Res Lett (USA)*, 19 (1992) 429.
- [2]. Cliver, E.W., *Solar Phys.*, 84 (1983) 347.
- [3]. Cane, H.V., McGuire, R. E. and Von Rosenvinge, T. T., *Astrophysical J.*, 301 (1986) 448.
- [4]. Gopalswamy, N., *The Sun and the Heliosphere as an Integrated System*, edited by Poletto, G. and Suess, S. T., Chap. 8 (2004) p 201, Kluwer Acad., Boston.
- [5]. Gopalswamy, N., Yashiro, S. and Akiyama, S., *J. Geophysics. Res.*, 112 (2007) A06112.
- [6]. Howard, R. A., Michels, D. J., Sheeley, N. R.(Jr.) and Kooman, M. J., *ApJ*, 263 (1982) L101.
- [7]. Forbush, S.E., *Phy. Rev.*, 70 (1946) 771.
- [8]. Kahler, S.W., 1992, *Annu. Rev. Astron. Astrophys.*, **30**, 113.
- [9]. Russell C T & McPherron R L, *Space Sci Rev (Netherlands)*, 15 (1973) L205.